Published in final edited form as:
Brain Dev. 2012 August ; 34(7): 553–562. doi:10.1016/j.braindev.2011.10.004.

A PERFUSION-METABOLIC MISMATCH IN STURGE-WEBER SYNDROME: A MULTIMODALITY IMAGING STUDY

Bálint Alkonyi, MD[1,2], **Yanwei Miao, MD, PhD**[3,5], **Jianlin Wu, MD, PhD**[3,5], **Zhaocheng Cai, MS**[3], **Jiani Hu, PhD**[3], **Harry T. Chugani, MD**[1,2,4], and **Csaba Juhász, MD, PhD**[1,2,4]

[1]Positron Emission Tomography Center, Children's Hospital of Michigan, Detroit, MI, USA

[2]Carman and Ann Adams Department of Pediatrics, Wayne State University School of Medicine, Detroit, MI, USA

[3]Department of Radiology, Wayne State University School of Medicine, Detroit, MI, USA

[4]Department of Neurology, Wayne State University School of Medicine, Detroit, MI, USA

[5]Department of Radiology, First Affiliated Hospital, Dalian Medical University, Dalian, Liaoning, China

Abstract

OBJECTIVE—We combined perfusion weighted imaging (PWI) with 2-deoxy-2[^{18}F]fluoro-D-glucose (FDG) positron emission tomography (PET) to study the relationship between regional metabolic and perfusion abnormalities and their clinical correlates in children with Sturge-Weber syndrome (SWS).

METHODS—Fifteen children (age: 0.9-10 years) with unilateral SWS underwent high-resolution PWI and FDG PET prospectively. Regional (lobar) asymmetry indices (AIs) of subcortical white matter (WM) cerebral blood flow (CBF) were correlated with corresponding cortical FDG uptake asymmetries, extent of leptomeningeal vascular malformation and clinical seizure variables.

RESULTS—Abnormal cortical glucose metabolism and/or subcortical WM CBF were seen in all lobes affected by vascular malformation and extended to lobes *not* affected by abnormal pial vessels in 6 patients. Lower CBF was associated with lower cortical glucose metabolism in the temporal, parietal and occipital lobes ($p \leq 0.02$). While decreased perfusion was associated with hypometabolism in most cases, i*ncreased* regional CBF (found in 6 patients) was commonly associated with relatively mild or no hypometabolism. Ten of 24 cerebral lobes with normal glucose metabolism in the affected hemisphere showed abnormal perfusion. High seizure frequency was associated with severe parieto-occipital hypoperfusion ($p \leq 0.03$), while long duration of epilepsy was related to frontal lobe hypometabolism ($p=0.015$).

CONCLUSIONS—Regional perfusion and cortical metabolic abnormalities can extend beyond lobes affected by leptomeningeal vascular malformations and are related to epilepsy in SWS.

Corresponding author: Csaba Juhász, MD, PhD Departments of Pediatrics and Neurology, Wayne State University PET Center, Children's Hospital of Michigan 3901 Beaubien St., Detroit, MI, 48201 Phone: 313-966-5136 Fax: 313-966-9228 juhasz@pet.wayne.edu.

CONFLICT OF INTEREST STATEMENT
We declare that the authors have no conflict of interest.

Despite a general correlation between perfusion and metabolism, increased WM perfusion with preserved cortical metabolism in overlying cortex is a common pattern of a perfusion/metabolic mismatch. This may represent a disease stage where cortical function is preserved while increased WM perfusion provides collateral drainage of cortex via the deep vein system.

Keywords

Sturge-Weber syndrome; MRI; perfusion weighted imaging; cerebral blood flow; positron emission tomography; glucose metabolism; epilepsy; children

1. Introduction

Sturge-Weber syndrome (SWS) is a congenital disorder characterized by facial cutaneous capillary malformation (port wine stain), leptomeningeal vascular malformation and glaucoma [1]. The leptomeningeal malformation, which is most common in the parieto-occipital regions and is unilateral in more than 80% of the cases [2], leads to abnormal cortical and subcortical drainage and venous stasis resulting in regional cerebral perfusion deficits and tissue hypoxia [3-5]. Neurological manifestations of SWS vary widely; however, seizures, stroke-like episodes, hemiparesis, hemianopia and cognitive impairment are frequently present [1].

Post-contrast T1-weighted MR images can delineate the extent of leptomeningeal malformation overlying the surface of the cortex [6]. Atrophy, calcification, enlarged deeps veins and choroid plexus are also common findings on conventional MRI. Functional imaging techniques are able to identify brain functional abnormalities extending beyond apparent structural involvement and provide assessment of dysfunction involving cortex, white matter (WM) and deep gray matter structures in SWS. Dynamic MR perfusion weighted imaging (PWI) studies in SWS have demonstrated perfusion deficits in brain regions underlying the leptomeningeal malformation [7]. Although the direct clinical implications of the decreased perfusion are unclear, one study suggested that larger hypoperfused tissue volumes may be associated with more severe hemiparesis in SWS [8]. It has been hypothesized that both chronic ischemia and epilepsy may contribute to regional hypoperfusion [9]. Decreased cortical glucose metabolism, detected by glucose positron emission tomography (PET), is another common imaging finding in patients with SWS. Hypometabolic regions are common in atrophic cortex but can also extend into cortex showing no structural abnormalities [3, 10-11]. Cortical hypometabolism may be secondary to underlying tissue hypoperfusion and hypoxia; however, no previous studies analyzed perfusion and glucose metabolic changes in the same patients with SWS.

Although decreased blood flow and glucose metabolism are the most common functional imaging findings in SWS, several studies reported interictal *increases* of both regional cerebral perfusion and glucose metabolism, particularly in some young children in the early stage of SWS [3, 12-15]. The exact mechanisms and clinical significance of these seemingly paradoxical phenomena are not known. There is no evidence that these increases are caused by ongoing seizures (since they were reported in the interictal state). Limited longitudinal data suggested that the increases in perfusion and metabolism are transient and switch to decreased perfusion and metabolism during the course of the disease [12-13, 16].

Since the above detailed perfusion and metabolic changes may be the key to understand pathophysiology of SWS, we examined regional (lobar) perfusion and glucose metabolic abnormalities in children with unilateral SWS using a combination of perfusion MRI and interictal glucose PET. We aimed to determine if perfusion and glucose metabolic abnormalities extend beyond the lobe affected by the vascular malformation, and if there is a

quantitative relationship between perfusion abnormalities and glucose metabolism measured in the same brain regions. We also analyzed if *increased* perfusion in the affected hemisphere is associated with glucose metabolic abnormalities. We hypothesized that abnormal perfusion can extend beyond cortical hypometabolism and vice versa, i.e., there is a perfusion/metabolic mismatch in certain brain regions of children with SWS. Finally, we analyzed whether clinical epilepsy variables (seizure frequency or duration of epilepsy) are related to specific regional perfusion or glucose metabolism abnormalities.

2. Subjects

In this study, data from 15 children (mean age: 4.4 years; range: 0.9-10 years; 9 females) with unilateral SWS were analyzed (**Table 1**). They were selected from a series of 45 children recruited prospectively for a clinical and neuroimaging study of children with SWS between 2003 and 2010. The inclusion of patients was based on the following criteria: (1) clinical and radiological diagnosis of SWS with unilateral intracranial involvement (leptomeningeal angioma) based on imaging features (conventional contrast-enhanced MRI as well as FDG PET), with or without facial angioma (patients with only intracranial angioma are classified as having type III SWS [17]), (2) the availability of good quality high-resolution PWI images and (3) the availability of FDG PET scans performed within 1 day before or after the MRI. Patients with bilateral brain involvement (on MRI and/or PET) were not included. Of the 15 children, 14 had a history of seizures, and all 14 took various antiepileptic drugs in mono or polytherapy; the only patient with no seizures had both facial and leptomeningeal angioma. Duration of epilepsy ranged from 2 months to 10 years. Only two children (#1 and 5 in **Table 1**) had a clinical seizure within 24 hours before the MRI (2 hours and 12 hours before MRI, respectively). To estimate seizure frequency, a seizure frequency score was calculated based on a scoring system proposed by Engel et al [18]. In the present study a simplified version of this scoring system (better suited for this patient group [15]) was used according to a 5-point scale as follows: 1: <1 seizure per year; 2: 1-11 seizures per year; 3: 1-3 seizure(s) per month; 4: 1-6 seizure(s) per week; 5: ≥1 seizure(s) per day. Hemispheric (but not lobar) white matter PWI data of all but one patient (patient #15) were reported in our recent study [15]. The study was approved by the Human Investigation Committee at Wayne State University, and written informed consent of the parent or legal guardian as well as verbal assent (from children age 7 and above) was obtained in all patients.

3. Methods

3.1. MR imaging protocol

The MRI examinations were carried out using a Sonata 1.5 T MR scanner (Siemens, Erlangen, Germany) with a standard head coil, as described previously [15]. Patients younger than 7 years of age were sedated with pentobarbital (3 mg/kg) followed by fentanyl (1μg/kg). The MRI protocol included an axial 3D gradient-echo T1-weighted acquisition, an axial T2-weighted turbo spin-echo acquisition, susceptibility weighted imaging (SWI), followed by dynamic contrast enhanced high-resolution MR perfusion-weighted imaging (HR-PWI) and a postgadolinium T1-weighted acquisition (using the same imaging parameters as the first T1 weighted acquisition) in all patients. The HR-PWI data were obtained using a two-dimensional gradient echo EPI sequence with TR = 2200 ms, TE = 98ms, flip angle = 60°, slice thickness = 4 mm. The field of view was 256 mm × 256 mm and matrix was 512×512. The scan was run 50 times. Gadolinium-DTPA (Magnevist, Berlex, USA) was injected in a bolus via a peripheral vein with a dose of 0.1 mmol/kg of body weight. On PWI, a smaller voxel size of 0.5×0.5×4.0 mm^3, as compared to those published previously [7, 19], was obtained to improve the ability of detecting subtle

structures in cerebral parenchyma; therefore, the PWI method used here is termed high-resolution.

3.2. FDG PET scanning protocol

The details of FDG-PET acquisition and data analysis have been described previously [20]. In brief, all PET scans were acquired using an EXACT/HR PET scanner (CTI/Siemens, Hoffman Estates, Ill), which provides simultaneous acquisition of 47 contiguous transaxial images with a slice thickness of 3.125 mm. The reconstructed image resolution obtained was 5.5±0.35 mm at full width at half-maximum in-plane and 6.0±0.5 mm at full width at half-maximum in the axial direction (reconstruction: filtered backprojection using Shepp-Logan filter with 0.3 cycles/pixel cutoff frequency). Scalp EEG was monitored in all children during the tracer uptake period. Initially, 5.29 MBq/kg of FDG was injected intravenously as a slow bolus followed by a 30 minutes uptake period. A static 20-minute emission scan was acquired parallel to the canthomeatal plane. Calculated attenuation correction was applied to the brain images using automated threshold fits to the sonogram data [21].

3.3. PWI analysis

Post-processing of PWI data has been described previously in our recent publication [15]. Perfusion parameter maps, including cerebral blood flow (CBF) maps were derived from raw MR perfusion data based on tracer kinetic methods [22-23] using a software developed in-house (Signal Process in Neuroradiology; SPIN). Deconvolution with singular value decomposition (SVD) was used to create quantitative CBF maps [22-23]. CBF values in the subcortical WM of all lobes and also in contralateral homotopic WM regions were measured. Analysis of WM, rather than cortex, had the advantage of avoiding artifacts from the low-flow leptomeningeal vascular malformation (which directly overlays affected cortical regions) as well as cortical calcification. In order to determine if subcortical WM and cortical CBF values are tightly correlated, cortical regions were also evaluated in the frontal lobe of all 9 patients whose frontal lobe was not affected by the angioma (and showed no calcification either). At least three regions of interest (ROIs), 20-40 voxels in size, were placed on representative slices in each lobe and also on homotopic contralateral WM (and frontal cortex for the selected 9 patients) by one of the investigators, who was blinded to the PET results and clinical variables. The reliability of these perfusion measurements obtained by manual ROI placement has been demonstrated previously [15]. On the CBF map, vessels and cortex appear red and green respectively, while WM has a blue color, allowing for accurate placement of ROIs over WM, while avoiding inclusion of cortex, ventricles or large vessels (dilated veins) within the white matter. Perfusion parameters were measured in not only affected (areas of leptomeningeal vascular malformation and/or dilated transmedullary veins) but also in apparently normal lobes. Lobar WM CBF asymmetry indices (AI) were calculated based on the following formula:

$$\text{CBF} \quad \text{AI} = (\text{CBF}_I - \text{CBF}_C) / [(\text{CBF}_I + \text{CBF}_C)/2],$$

where CBF_I indicates the CBF values in WM ipsilateral to the vascular malformation, and CBF_C is the perfusion value in the contralateral hemisphere, measured in the homotopic region. The use of asymmetry indices, rather than absolute perfusion values, was beneficial so that the effect of considerable, non-linear age-dependent variations of brain perfusion in children [24-25] could be largely eliminated.

3.4. FDG PET analysis

To quantify glucose metabolism in each cerebral lobe, an ROI approach was implemented. Representative cortical areas of all 4 lobes in the affected hemisphere were outlined in at

least 3 slices using the software ROI Editor (www.mristudio.org) by one of the investigators (B.A.), who was blinded to the PWI results. In addition, ROIs of similar size were also placed on contralateral homotopic cortical areas. Subsequently, standardized uptake values (SUVs) were calculated as the ratio between the average radioactivity concentration obtained from each region and the injected dose per weight (MBq/kg). Finally, SUV asymmetry indices (AIs) were calculated using the following formula:

$$\text{FDG AI} = (\text{FDG}_I - \text{FDG}_C) / [(\text{FDG}_I + \text{FDG}_C)/2],$$

where FDG_I represents ipsilateral and FDG_C represents contralateral cortical FDG SUVs. Again, the use of asymmetry indices, rather than absolute FDG SUV values, was beneficial so that the effect of considerable, non-linear age-dependent variations of brain glucose metabolism in children could be eliminated [26]. Asymmetries are also much less sensitive to global effects of antiepileptic drugs on brain glucose metabolic values.

3.5. Study design and statistical analysis

Initially, we assessed the spatial association between the location of leptomeningeal vascular malformation (by lobe), defined on T1-weighted post-gadolinium MRI and corresponding quantitative PWI as well as FDG PET abnormalities. Lobes with increased and decreased CBF values and FDG SUVs, on the affected side, were identified based on a 10% asymmetry (i.e., AI= 0.10) limit. This asymmetry limit was selected based on previous pediatric brain MRI perfusion and FDG PET studies suggesting that lobar perfusion and glucose metabolism asymmetries above 10% can be considered abnormal [19, 27]. In a previous study of children with SWS, we have also shown that FDG asymmetries of 10-20% (i.e., AI between 0.10 and 0.20) corresponds to mildly hypometabolic but structurally preserved cortex (no atrophy or calcification), while AI>0.20 indicates severe hypometabolism likely representing atrophic cortex [20]. Based on the 0.10 AI threshold, all lobes in the affected hemisphere were classified as showing increased, normal and decreased perfusion and/or glucose metabolism, and these classifications were used to identify lobes with a perfusion/metabolic mismatch (defined as having a discrepancy between perfusion vs. metabolism classification of the same lobe). Non-parametric Spearman's rank correlations were performed between corresponding WM and cortical CBF values (in the 9 patients where frontal cortical measurements were done) and also between corresponding lobar AI values of CBF and FDG SUV AIs. This analysis was also repeated for each lobe separately with corresponding measurements. Finally, seizure frequency scores and the duration of epilepsy were correlated with AIs of CBF as well as FDG SUVs for each lobe, using Spearman's rank correlation. Statistical analysis was carried out using the software SPSS Statistics 19.0 (IBM Co., Somers, NY). Since multiple correlations have been carried out, a conservative $p<0.01$ was considered as the limit of significance.

4. Results

4.1. Location of vascular malformation vs. quantitative FDG PET/PWI abnormalities

T1-weighted post-gadolinium MRI demonstrated that leptomeningeal malformations affected 39 of the 60 cerebral lobes (in affected hemispheres) in the 15 patients (**Table 1**). All 39 affected lobes showed abnormal perfusion, abnormal glucose metabolism or both. In addition, abnormal glucose metabolism and/or CBF in lobes *not* affected by pial vascular malformation were seen in 6 patients (glucose hypometabolism in 5 patients and abnormal CBF in 3; **Table 1**).

4.2. Correlation between WM and cortical perfusion in the frontal lobe

In the 9 patients with no frontal angioma, there was a strong correlation between subcortical WM and corresponding cortical CBF values (ipsilateral frontal lobe: Spearman's rho = 0.91; contralateral frontal lobe: Spearman's rho = 0.89; $p<0.001$ in both correlations). This indicated that subcortical WM CBF values could be good indicators of cortical perfusion even in patients (and lobes) where direct measurement of cortical perfusion was not done because of the confounding effect of the overlying angioma.

4.3. Correlation between WM perfusion and cortical glucose metabolism asymmetries

There was a general positive correlation between hemispheric mean subcortical WM CBF and FDG AI values [$r=0.60$, $p<0.0001$; see **Figure 1**], with similar significant correlations in corresponding temporal and parietal lobe values ($p<0.01$; **Table 2**). Weaker CBF AI vs. FDG AI correlations were found in the occipital lobe ($p=0.02$); frontal lobe FDG and perfusion asymmetries did not correlate with each other ($p=0.48$).

4.4. Perfusion vs. metabolic abnormalities in individual patients

At least one lobe with *decreased* CBF was present in 9 patients (mean CBF AI: -42%, in a total of 28 lobes: parietal: 9, occipital: 8, temporal: 7, frontal: 4), and overlying cortex was commonly hypometabolic in these regions (**Figure 2B**; mean FDG AI: -43.3%; range: -97 - +10%; only 3 of these 28 affected lobes showed normal cortical glucose metabolism) (**Table 3**).

Increased CBF was observed in 6 patients (mean CBF AI: 30.3% in a total of 14 lobes: frontal: 3, parietal: 5, temporal: 3, occipital: 3) and was associated with relatively mild or no hypometabolism on PET in most cases (**Figure 2A**; mean FDG AI: -11.1%; range: -44 - +11%; normal FDG AI in 7/14 lobes; only 4 of the 14 lobes showed severe [AI>0.20] hypometabolism).

Normal CBF was observed in 18 lobes (frontal: 8, temporal: 5, occipital: 4, parietal: 1) of 9 patients. Four of these regions showed decreased cortical glucose metabolism and 14 showed normal metabolism (mean FDG AI: -5.7 %).

Altogether 24 lobes in 12 children showed normal glucose metabolism (although all children had abnormal glucose metabolism in at least one lobe). Among the normometabolic regions, 10 lobes (42%) of 8 patients had abnormal CBF AI (increased CBF in 7 lobes and decreased CBF in 3 lobes).

In total, a perfusion/metabolism mismatch was seen in 20 lobes of 11 patients, most commonly in lobes (n=13) showing increased WM CBF. Various types of perfusion/metabolism mismatch are summarized in **Table 3**.

4.5. Correlations between imaging and seizure variables

High frequency of seizures was associated with severe parietal and occipital CBF decreases ($r=-0.64$, $p=0.01$; $r=-0.56$, $p=0.03$, respectively). We also found a significant inverse correlation between seizure frequency scores and occipital glucose metabolism asymmetry ($r=-0.69$, $p=0.005$) as well as a similar trend for association between seizure frequency scores and parietal hypometabolism ($r=-0.55$, $p=0.034$). Longer epilepsy duration showed a moderate correlation with frontal FDG AI ($r=-0.61$, $p=0.015$). Duration of epilepsy did not correlate with CBF AI of any lobes.

5. Discussion

This multimodality imaging study shows that both subcortical white matter perfusion and cortical glucose metabolic abnormalities can extend beyond the lobe affected by the leptomeningeal vascular malformation. Despite a general association between these perfusion and metabolic abnormalities, a regional perfusion/metabolism mismatch is also often present in children with SWS. The most common mismatch pattern occurred in lobes with *increased* subcortical white perfusion that often showed normal glucose metabolism or only mild hypometabolism in overlying cortex. Furthermore, high seizure frequency seems to be related to decreased perfusion and hypometabolism in the posterior brain regions (the most common sites of the leptomeningeal vascular malformation), whereas longer duration of epilepsy is associated with hypometabolism of frontal areas, which are often not involved in primary pathology but become affected as the disease progresses.

5.1.The classic pattern of cerebral hypoperfusion and hypometabolism in SWS

In general, previous SPECT, xenon-CT, PWI and PET studies all showed that hypoperfusion and hypometabolism are the most common abnormalities in the affected area of patients with SWS and chronic epilepsy [3, 8-9, 28-29]. Importantly, previous cerebral blood flow SPECT and FDG PET studies showed that perfusion and metabolic abnormalities are anatomically well matched with the region of the vascular malformation; however, the perfusion and metabolic deficit can extend beyond the lobe with overlying leptomeningeal enhancement [3, 9]. This observation is now further supported by our results showing brain regions with abnormal perfusion and/or glucose metabolism in lobes not affected by the malformation. With respect to metabolic aspects of compromised perfusion, reduced NAA levels, indicating cell dysfunction and neuronal loss, were seen in hypoperfused brain tissue of patients with SWS [8]. Also, a SPECT study addressed the hypothesis that decreased perfusion may mediate neurological dysfunction by altering cellular glucose metabolism [30]. In most cases with focal hypoperfusion, cerebral glucose metabolism was decreased at some point of the follow-up. Concordantly, here we demonstrate that more severe cortical hypometabolism is associated with decreased blood flow in the underlying WM. Still, we observed decreased FDG uptake in lobes showing normal CBF and vice versa in a few cases, although FDG decreases in lobes with normal perfusion were rare (n=4) and moderate (12-18% decrease).

5.2. Perfusion/metabolism mismatch and increased perfusion

A novel finding of the present study is that a spatial perfusion/metabolic mismatch is common in individual patients with SWS: in particular, subcortical WM perfusion was often increased under normometabolic or mildly hypometabolic cortical regions. Since SWS is a clinical model of early brain damage resulting from chronic tissue hypoxia, it is difficult to find analogous diseases that could provide clues for the understanding of this discrepancy. *Hyper*perfusion is often seen in neonatal hypoxic-ischaemic encephalopathy [31-32], which develops after an acute, usually global, ischemic event. Still, increased perfusion of the cortex can persist in the subacute phase in affected neonates [31]. Transient *hyper*perfusion can also occur in epilepsy patients in the periictal period [33]. However, most of our patients (13 of 15) had no seizure on the day of MRI or PET scanning. A SPECT study demonstrated that *increased* perfusion may be present in infants with SWS even before the onset of first seizures [12]. Similarly, a paradoxical phenomenon of a transient, interictal *hyper*metabolism has been described in young patients with SWS and recent onset seizures or even before the first seizure [3, 13, 14], possibly indicating a transient phase of hypoxic, excitotoxic damage related to epileptogenesis. Transient increase of glucose metabolism, also described in young children with hypoxic damage after perinatal hypoxia, may be a marker of hypoxia-induced, glutamatergic excitotoxic injury leading to subsequent

hypometabolism [34-36]. In the present study, *increased* perfusion was *not* accompanied by increased cortical glucose metabolism (with the one exception of the parietal lobe of patient #12, the only patient with no epilepsy). Therefore, it is likely that increased perfusion and glucose metabolism are due to different mechanisms or occur in different stages of the disease.

5.3. Implications for epilepsy

There were two major findings relating perfusion/metabolic abnormalities to epilepsy. First, frequent seizures were associated with more severe perfusion abnormalities in the posterior areas, the typical sites of vessel abnormalities and early structural damage in SWS. Since frequent seizures can have detrimental effects on brain tissue due to transient focal increases in oxygen and metabolic demand (which cannot be met in poorly perfused brain tissue), it is likely that frequent seizures, originated from posterior regions, may contribute to progression of brain damage to more anterior regions during the course of the disease. This is supported by a recent longitudinal glucose PET study showing a progressive enlargement of cortical hypometabolism in SWS children with frequent seizures [37]. Second, we also found a moderate correlation between longer epilepsy duration and glucose hypometabolism in the frontal lobe. This suggests a progressive involvement and deterioration of the frontal regions, which are often less involved during the initial stages of the disease. Altogether, both findings suggest a detrimental effect of chronic seizures on brain perfusion and metabolism in SWS.

Based on our data and the above outlined recent studies we speculate that interictal white matter *hyper*perfusion with normal or close to normal glucose metabolism in overlying cortex indicates a disease stage where venous drainage of affected cortex is largely preserved via the deep venous system, thus compensating for insufficient venous outflow through the superficial veins. The failure of salvage mechanisms along with the deleterious effect of seizures may eventually lead to the classic ‘burn out’ pattern of hypometabolism coupled with hypoperfusion and atrophy. This process may occur at its own pace in different brain areas of patients and may not be directly associated with age.

5.4. Potential limitations

Our approach was designed to find associations between distinct functional measures (perfusion and glucose metabolism) of spatially related but different tissue types (WM and GM) of the brain. In order to obtain reliable measures of regional perfusion status, only white matter perfusion was measured, since calcification and vascular malformation-related blood flow changes in the cortex could have confounded our results. This was less of a concern in the subcortical white matter, where ROI placement was carefully performed to make sure that large transmedullary veins were avoided [15]. Also, impaired venous outflow due to abnormal surface veins should affect not only cortex but also underlying subcortical white matter, which is also normally drained via those superficial veins [38]. The strong correlations between cortical and subcortical WM CBF values in the frontal lobe of patients with no frontal angioma also supported that the measured WM perfusion changes reflected abnormalities in the overlying GM accurately in most cases.

Due to age-related changes in cerebral perfusion and metabolism during early childhood, the use of asymmetries (AIs), rather than absolute perfusion/metabolic values, is useful to minimize concern regarding age-related changes in absolute measures [24-26]. This approach is also beneficial to eliminate variable effects of various antiepileptic drugs on brain glucose metabolism. Although minor functional demise of the contralateral hemisphere cannot be ruled out, none of our patients had bilateral involvement on

conventional post-contrast MRI, and none of them showed focal cortical hypometabolism on PET upon visual evaluation.

Finally, one could argue that some of the observed perfusion/metabolism mismatches are simply due to the applied asymmetry thresholds. We used a uniform 10% asymmetry threshold for both FDG and CBF asymmetries for simplicity and based on previous studies in normal children (for PWI) and children with SWS (for FDG PET) [20, 27]. Still, the exact limit for abnormal asymmetries may be different for the two imaging modalities and may slightly vary across ages and lobes. However, if we reanalyze our data using different CBF AI thresholds (using either a 5%, 15% or even 20% asymmetry threshold), the major results, indicating a common association between increased perfusion and decreased or normal glucose uptake, would hardly change, as all but one CBF AI values in this subgroup were above 0.20 (i.e., more than 20% asymmetry). Therefore, we are confident that the reported mismatch pattern is not an artifact of asymmetry threshold selection.

5.5. Conclusion

In conclusion, in this study we demonstrated a general correlation between regional white matter hypoperfusion, seizure severity and cortical glucose hypometabolism in children with SWS. We also found a regional perfusion/metabolic mismatch in individual patients. This may indicate areas that are at risk for future metabolic and functional deterioration. This could be assessed in future longitudinal imaging studies.

Acknowledgments

This study was supported by a grant from the National Institutes of Health (R01 NS041922). The content is solely the responsibility of the authors and does not necessarily represent the official views of the NIH. We are grateful to Majid Khalaf, MD, Anne Deboard, RN and Jane Cornett, RN for their assistance in sedation. The authors thank Thomas Mangner, PhD, and Pulak Chakraborty, PhD, for the reliable radiosynthesis of FDG, Yang Xuan, BS, for MR image acquisitions, as well as Michael Behen ,PhD, William Guy, and Stacey Halverson for neuropsychology testing. We are also grateful to Galina Rabkin, CNMT, Angie Wigeluk, CNMT, and Carole Klapko, CNMT, for their expert technical assistance in performing the PET studies. We thank the Sturge-Weber Foundation for referring patients to us. We are also grateful to the families and children who participated in the study.

REFERENCES

1. Bodensteiner, JB.; Roach, ES. Overview of Sturge-Weber syndrome.. In: Bodensteiner, JB.; Roach, ES., editors. Sturge-Weber syndrome. p. 19-32.
2. Comi, AM.; Roach, ES.; Bodensteiner, JB. Neurological manifestations of Sturge-Weber syndrome.. In: Bodensteiner, JB.; Roach, ES., editors. Sturge-Weber Syndrome. Mt Freedom; The Sturge-Weber Foundation; NJ: 2010. p. 69-93.
3. Chugani HT, Mazziotta JC, Phelps ME. Sturge-Weber syndrome: a study of cerebral glucose utilization with positron emission tomography. J Pediatr. 1989; 114:244–53. [PubMed: 2783735]
4. Reid DE, Maria BL, Drane WE, Quisling RG, Hoang KB. Central nervous system perfusion and metabolism abnormalities in Sturge-Weber syndrome. J Child Neurol. 1997; 12:218–22. [PubMed: 9130099]
5. Okudaira Y, Arai H, Sato K. Hemodynamic compromise as a factor in clinical progression of Sturge-Weber syndrome. Childs Nerv Syst. 1997; 13:214–9. [PubMed: 9202857]
6. Thomas-Sohl KA, Vaslow DF, Maria BL. Sturge-Weber syndrome: a review. Pediatr Neurol. 2004; 30:303–10. [PubMed: 15165630]
7. Evans AL, Widjaja E, Connolly DJ, Griffiths PD. Cerebral perfusion abnormalities in children with Sturge-Weber syndrome shown by dynamic contrast bolus magnetic resonance perfusion imaging. Pediatrics. 2006; 117:2119–25. [PubMed: 16740855]
8. Lin DD, Barker PB, Hatfield LA, Comi AM. Dynamic MR perfusion and proton MR spectroscopic imaging in Sturge-Weber syndrome: correlation with neurological symptoms. J Magn Reson Imaging. 2006; 24:274–81. [PubMed: 16786573]

9. Chiron C, Raynaud C, Tzourio N, Diebler C, Dulac O, Zilbovicius M, et al. Regional cerebral blood flow by SPECT imaging in Sturge-Weber disease: an aid for diagnosis. J Neurol Neurosurg Psychiatry. 1989; 52:1402–9. [PubMed: 2614436]
10. Juhasz C, Haacke EM, Hu J, Xuan Y, Makki M, Behen ME, et al. Multimodality imaging of cortical and white matter abnormalities in Sturge-Weber syndrome. AJNR Am J Neuroradiol. 2007; 28:900–6. [PubMed: 17494666]
11. Alkonyi B, Chugani HT, Behen M, Halverson S, Helder E, Makki MI, et al. The role of the thalamus in neuro-cognitive dysfunction in early unilateral hemispheric injury: a multimodality imaging study of children with Sturge-Weber syndrome. Eur J Paediatr Neurol. 2010; 14:425–33. [PubMed: 20447845]
12. Pinton F, Chiron C, Enjolras O, Motte J, Syrota A, Dulac O. Early single photon emission computed tomography in Sturge-Weber syndrome. J Neurol Neurosurg Psychiatry. 1997; 63:616–21. [PubMed: 9408103]
13. Alkonyi B, Chugani HT, Juhasz C. Transient focal cortical increase of interictal glucose metabolism in Sturge-Weber syndrome: Implications for epileptogenesis. Epilepsia. 2011; 52:1265–72. [PubMed: 21480889]
14. Al-Makhzomi M, Goffin K, De Waele L, Lagae L, Van Laere K, et al. Paradoxical interictal cerebral cortical hypermetabolism on brain FDG PET in Sturge-Weber syndrome. Clin Nucl Med. 2011; 36:313–4. [PubMed: 21368611]
15. Miao Y, Juhasz C, Wu J, Tarabishy B, Lang Z, Behen ME, et al. Clinical correlates of white matter blood flow perfusion changes in Sturge-Weber syndrome: A dynamic MR perfusion-weighted imaging study. AJNR Am J Neuroradiol. 2011; 32:1280–5. [PubMed: 21724573]
16. Freilinger T, Peters N, Remi J, Linn J, Hacker M, Straube A, et al. A case of Sturge-Weber syndrome with symptomatic hemiplegic migraine: clinical and multimodality imaging data during a prolonged attack. J Neurol Sci. 2009; 287:271–4. [PubMed: 19733861]
17. Roach ES. Neurocutaneous syndromes. Pediatr Clin North Am. 1992; 39:591–620. [PubMed: 1635798]
18. Engel, JJ.; Van Ness, PC.; Rasmussen, TB.; Ojemann, LM. Outcome with respect to epileptic seizures.. In: Engel, JJ., editor. Surgical treatment of the epilepsies. 2nd ed.. Raven P; New York: p. 609-21.
19. Oguz KK, Senturk S, Ozturk A, Anlar B, Topcu M, Cila A. Impact of recent seizures on cerebral blood flow in patients with Sturge-Weber syndrome: study of 2 cases. J Child Neurol. 2007; 22:617–20. [PubMed: 17690070]
20. Lee JS, Asano E, Muzik O, Chugani DC, Juhasz C, Pfund Z, et al. Sturge-Weber syndrome: correlation between clinical course and FDG PET findings. Neurology. 2001; 57:189–95. [PubMed: 11468301]
21. Bergstrom M, Litton J, Eriksson L, Bohm C, Blomqvist G. Determination of object contour from projections for attenuation correction in cranial positron emission tomography. J Comput Assist Tomogr. 1982; 6:365–72. [PubMed: 6978896]
22. Ostergaard L, Weisskoff RM, Chesler DA, Gyldensted C, Rosen BR, et al. High resolution measurement of cerebral blood flow using intravascular tracer bolus passages. Part I: Mathematical approach and statistical analysis. Magn Reson Med. 1996; 36:715–25. [PubMed: 8916022]
23. Ostergaard L, Sorensen AG, Kwong KK, Weisskoff RM, Gyldensted C, Rosen BR, et al. High resolution measurement of cerebral blood flow using intravascular tracer bolus passages. Part II: Experimental comparison and preliminary results. Magn Reson Med. 1996; 36:726–36. [PubMed: 8916023]
24. Wang J, Licht DJ, Jahng GH, Liu CS, Rubin JT, Haselgrove J, et al. Pediatric perfusion imaging using pulsed arterial spin labeling. J Magn Reson Imaging. 2003; 18:404–13. [PubMed: 14508776]
25. Biagi L, Abbruzzese A, Bianchi MC, Alsop DC, Del Guerra A, Tosetti M. Age dependence of cerebral perfusion assessed by magnetic resonance continuous arterial spin labeling. J Magn Reson Imaging. 2007; 25:696–702. [PubMed: 17279531]

26. Chugani HT, Phelps ME, Mazziotta JC. Positron emission tomography study of human brain functional development. Ann Neurol. 1987; 22:487–97. [PubMed: 3501693]
27. Taki Y, Hashizume H, Sassa Y, Takeuchi H, Wu K, Asano M, et al. Correlation between gray matter density-adjusted brain perfusion and age using brain MR images of 202 healthy children. Hum Brain Mapp. Jan 21.2011 10.1002/hbm.21163.
28. Griffiths PD, Boodram MB, Blaser S, Armstrong D, Gliday DL, Harwood-Nash D. 99mTechnetium HMPAO imaging in children with the Sturge-Weber syndrome: a study of nine cases with CT and MRI correlation. Neuroradiology. 1997; 39:219–24. [PubMed: 9106299]
29. Yu TW, Liu HM, Lee WT. The correlation between motor impairment and cerebral blood flow in Sturge-Weber syndrome. Eur J Paediatr Neurol. 2007; 11:96–103. [PubMed: 17317246]
30. Maria BL, Neufeld JA, Rosainz LC, Drane WE, Qusling RG, Ben-David K, et al. Central nervous system structure and function in Sturge-Weber syndrome: evidence of neurologic and radiologic progression. J Child Neurol. 1998; 13:606–18. [PubMed: 9881531]
31. Wintermark P, Moessinger AC, Gudinchet F, Meuli R. Temporal evolution of MR perfusion in neonatal hypoxic-ischemic encephalopathy. J Magn Reson Imaging. 2008; 27:1229–34. [PubMed: 18504740]
32. Wintermark P, Moessinger AC, Gudinchet F, Meuli R. Perfusion-weighted magnetic resonance imaging patterns of hypoxic-ischemic encephalopathy in term neonates. J Magn Reson Imaging. 2008; 28:1019–25. [PubMed: 18821602]
33. Van Paesschen W, Dupont P, Sunaert S, Goffin K, Van Laere K. The use of SPECT and PET in routine clinical practice in epilepsy. Curr Opin Neurol. 2007; 20:194–202. [PubMed: 17351491]
34. Blennow M, Ingvar M, Lagercrantz H, Stone-Elander S, Eriksson L, Forssberg H, et al. Early [^{18}F]FDG positron emission tomography in infants with hypoxic-ischaemic encephalopathy shows hypermetabolism during the postasphyctic period. Acta Paediatr. 1995; 84:1289–95. [PubMed: 8580629]
35. Pu Y, Li QF, Zeng CM, Gao J, Qi J, Luo DX, et al. Increased detectability of alpha brain glutamate/glutamine in neonatal hypoxic-ischemic encephalopathy. AJNR Am J Neuroradiol. 2000; 21:203–12. [PubMed: 10669252]
36. Batista CE, Chugani HT, Juhasz C, Behen ME, Shankaran S. Transient hypermetabolism of the basal ganglia following perinatal hypoxia. Pediatr Neurol. 2007; 36:330–3. [PubMed: 17509466]
37. Juhasz C, Batista CE, Chugani DC, Muzik O, Chugani HT. Evolution of cortical metabolic abnormalities and their clinical correlates in Sturge-Weber syndrome. Eur J Paediatr Neurol. 2007; 11:277–84. [PubMed: 17408998]
38. Oka K, Rhoton AL Jr. Barry M, Rodriguez R. Microsurgical anatomy of the superficial veins of the cerebrum. Neurosurgery. 1985; 17:711–48. [PubMed: 4069326]

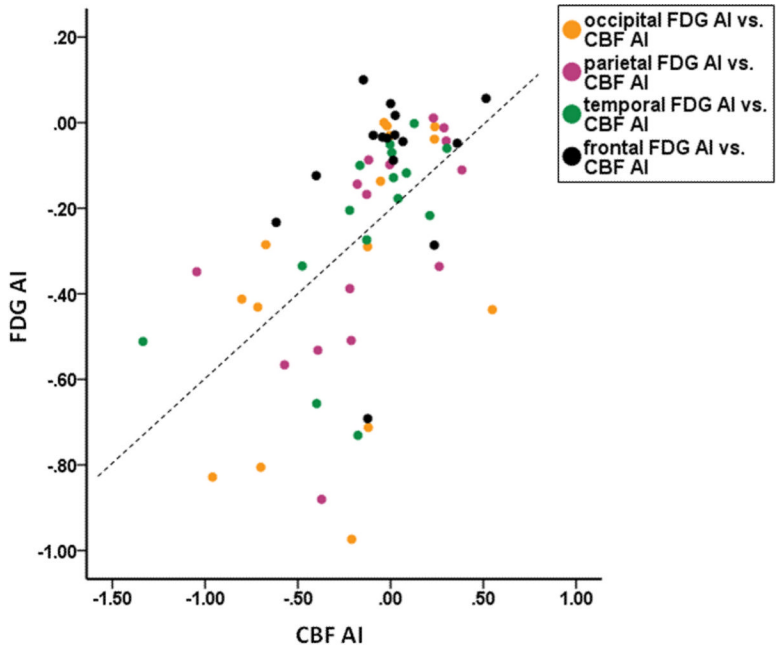

Figure 1.

Correlation between lobar white matter perfusion asymmetries and corresponding lobar cortical glucose metabolic asymmetries. Color code indicates the different lobes of the 15 patients, and the fitted regression line (dashed line; $r=0.60$, $p<0.0001$) assumes correlation between measurements of 60 lobes. FDG AI= cortical glucose metabolic asymmetry; CBF AI= cerebral blood flow asymmetry of the underlying white matter.

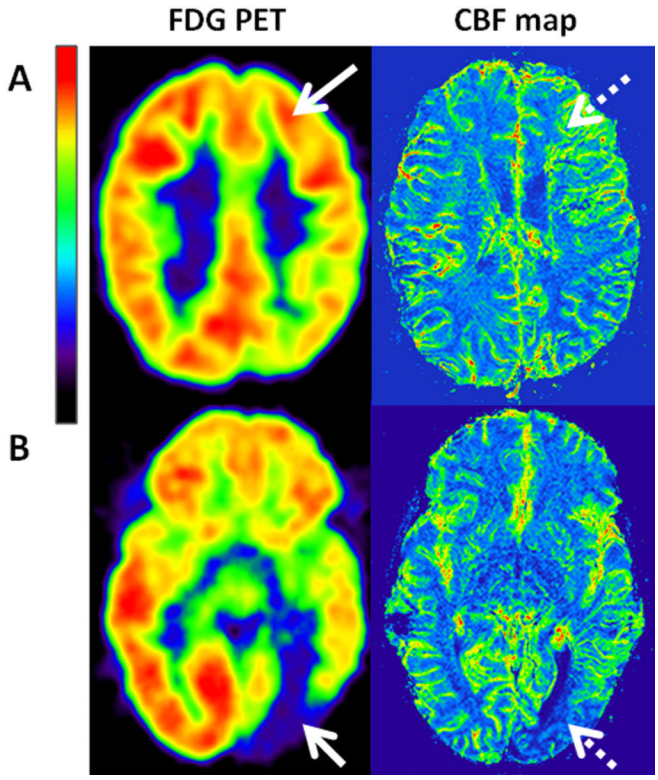

Figure 2.
Representative axial slices of FDG PET scans and cerebral blood flow (CBF) maps of two patients. Panel **A** depicts the normometabolic left frontal lobe (FDG AI=-5%; arrow) of patient #4. PWI demonstrated increased CBF (AI=36%) in the underlying white matter (dashed arrow). Panel **B** shows severe cortical glucose hypometabolism of the left occipital lobe (FDG AI= -97%; arrow) of patient #8 and concomitant decreased white matter perfusion in this area (CBF AI= -21%; dashed arrow).

Table 1

Clinical and quantitative imaging data of the patients.

Patient No./gender	Age (years)	Epilepsy duration (years)	Seizure frequency [score]	IQ	Location of vascular malformation	Occipital CBF AI/ *FDG AI*	Parietal CBF AI/ *FDG AI*	Temporal CBF AI/ *FDG AI*	Frontal CBF AI/ *FDG AI*
1/M	7.0	6.5	>10/day [5]	47	lFPO	**-0.80**/***-0.41***	**-1.04**/***-0.35***	**-0.13**/***-0.27***	**-0.62**/***-0.23***
2/F	2.0	1.9	1/year [2]	55	lFTPO	**-0.96**/***-0.83***	**-0.37**/***-0.88***	**-0.18**/***-0.73***	**-0.12**/***-0.69***
3/F	10.0	9.8	monthly [3]	55	lFTPO	**-0.72**/***-0.43***	**-0.57**/***-0.57***	**-1.34**/***-0.51***	**-0.40**/***-0.12***
4/F	5.0	4.5	<1/year [1]	117	lTO	**-0.67**/***-0.29***	**-0.18**/***-0.14***	**-0.48**/***-0.34***	**0.36**/***-0.05***
5/M	5.0	0.5	monthly [3]	99	rPO	**-0.12**/***-0.71***	**-0.21**/***-0.51***	**0.09**/***-0.12***	**0.00**/***0.04***
6/M	1.8	1.0	10/mo [4]	105	lTPO	**-0.70**/***-0.80***	**-0.39**/***-0.53***	**-0.40**/***-0.66***	**0.02**/***-0.09***
7/F	0.9	0.6	few/month [3]	not available	rFTPO	**-0.12**/**-0.29**	**-0.13**/***-0.17***	**-0.22**/***-0.21***	**-0.15**/***0.10***
8/M	4.0	0.5	weekly [4]	110	lPO	**-0.21**/***-0.97***	**-0.12**/***-0.08***	**0.04**/***-0.18***	**0.02**/***-0.03***
9/M	9.0	8.4	1/year [2]	93	lP	**-0.02**/***-0.01***	**-0.22**/***-0.39***	**-0.17**/***-0.10***	**0.07**/***-0.04***
10/F	1.6	1.0	few/year [2]	71	rFTPO	**0.55**/***-0.44***	**0.26**/***-0.34***	**0.21**/***-0.22***	**0.51**/***0.06***
11/M	1.8	0.2	few/year [2]	92	rTPO	**0.24**/***-0.04***	**0.38**/***-0.11***	**0.13**/***-0.00***	**0.03**/***0.02***
12/F	2.0	--	0 [1]	105	lTPO	**0.24**/***-0.01***	**0.23**/***0.11***	**0.30**/***-0.06***	**-0.02**/***-0.04***
13/F	4.0	2.0	<1/year [1]	102	lP	**-0.00**/***-0.03***	**0.30**/***-0.04***	**0.01**/***-0.07***	**-0.09**/***-0.03***
14/F	4.0	3.9	<1/year [1]	91	lFP	**-0.04**/***-0.00***	**0.29**/***-0.12***	**-0.00**/***-0.05***	**0.24**/***-0.29***
15/F	8.0	3.5	1/year [2]	101	rO	**-0.05**/***-0.14***	**-0.01**/***-0.10***	**0.02**/***-0.13***	**-0.04**/***-0.03***

Note: M: male, F: female, y: years, seizure frequency score definition: 1 if <1 seizure per year; 2 if 1-11 seizures per year; 3 if 1-3 seizure(s) per month; 4 if 1-6 seizure(s) per week; 5 if ≥1 seizure(s) per day; IQ: a measure of global intellectual functioning determined by age-appropriate tests; l: left, r: right, F: frontal, T: temporal, P: parietal, O: occipital, CBF: cerebral blood flow, FDG: 2-deoxy-2[^{18}F]fluoro-D-glucose, AI: asymmetry index; FDG AI refers to glucose SUV asymmetry of the corresponding lobe. AI = 2 × (I - C) / (I + C), where I refers to values measured in the affected (ipsilateral) hemisphere and C refers to those of the contralateral side. **Red** values indicate abnormal decreases and green values indicate abnormal increases of CBF and FDG uptake on the affected side. Values with yellow background indicate abnormal CBF or FDG uptake values in a lobe with no vascular malformation.

Table 2

Lobar perfusion and glucose metabolic asymmetries (mean± SD from 15 patients) and their correlations.

Mean ± SD	occipital	parietal	temporal	frontal
CBF AI	-0.23±0.44	-0.12±0.39	-0.14±0.39	-0.01±0.27
FDG AI	-0.35±0.34	-0.28±0.26	-0.24±0.22	-0.10±0.19
Correlations				
CBF AI vs. *FDG AI*	r=0.56; p=0.02	**r=0.79; p=0.001**	**r=0.65; p=0.008**	r=0.2; p=0.48

Note: SD: standard deviation; FDG: 2-deoxy-2[^{18}F]fluoro-D-glucose; AI: asymmetry index; CBF: cerebral blood flow; r: correlation coefficient (Spearman's); p: significance level.

Table 3

Types of perfusion/metabolism mismatch; number of lobes (number of patients in parentheses) is indicated for each type. A total of 10 patients showed at least one type of mismatch, including 4 with more than one type. Increased perfusion associated with normal or decreased glucose metabolism was the most common mismatch pattern.

		CBF		
		Decreased	**Normal**	**Increased**
FDG	**Decreased**	No mismatch	4 (3)	6 (3)
	Normal	3 (3)	No mismatch	7 (5)

Note: FDG: 2-deoxy-2[^{18}F]fluoro-D-glucose; CBF: cerebral blood flow